JACS
JOURNAL OF THE AMERICAN CHEMICAL SOCIETY

Article

pubs.acs.org/JACS

Designing Processive Catalytic Systems. Threading Polymers through a Flexible Macrocycle Ring

Alexander B. C. Deutman, Seda Cantekin, Johannes A. A. W. Elemans, Alan E. Rowan,* and Roeland J. M. Nolte*

Radboud University Nijmegen, Institute for Molecules and Materials, Heyendaalseweg 135, 6525 AJ, Nijmegen, The Netherlands

Supporting Information

ABSTRACT: The translocation of polymers through pores is widely observed in nature and studying their mechanism may help understand the fundamental features of these processes. We describe here the mechanism of threading of a series of polymers through a flexible macrocyclic ring. Detailed kinetic studies show that the translocation speed is slower than the translocation speed through previously described more rigid macrocycles, most likely as a result of the wrapping of the macrocycle around the polymer chain. Temperature-dependent studies reveal that the threading rate increases on decreasing the temperature, resulting in a negative activation enthalpy of threading. The latter is related to the opening of the cavity of the macrocycle at lower temperatures, which facilitates binding. The translocation process along the polymer chain, on the other hand, is enthalpically unfavorable, which can be ascribed to the release of the tight binding of the macrocycle to the chain upon translocation. The combined kinetic and thermodynamic data are analyzed with our previously proposed consecutive-hopping model of threading. Our findings provide valuable insight into the translocation mechanism of macrocycles on polymers, which is of interest for the development of processive catalysts, i.e., catalysts that thread onto polymers and move along it while performing a catalytic action.

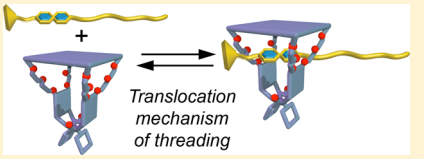

INTRODUCTION

DNA polymerase and λ-exonuclease are examples of naturally occurring rotaxane-like catalytic systems that bind to DNA and move along it, while performing a catalytic action, e.g., duplication or cleavage of the DNA strand. Catalysts of this type are called processive and are different from conventional catalytic systems, which convert substrate molecules in a distributive way, i.e., molecule by molecule in a random fashion without continuous attachment to a substrate.[1,2] Rotaxane-like architectures have also been shown to be essential for the transport of proteins across membranes and for the packaging and release of RNA and DNA through holes or openings in viruses.[3,4] In previous papers we reported that relatively simple molecules, comprising a glycoluril cage compound provided with a porphyrin roof (Figure 1a, compound **1**) can behave in a similar way as the above-mentioned processive enzyme systems. As a virtue of its toroidal shape, it can bind to linear polymer chains, which thread through its cavity.[5−7] The manganese(III) derivative of this porphyrin cage was found to epoxidize the alkene double bonds of a polybutadiene thread while gliding along it.[5,6] An important question to be answered was whether the catalytic oxidation of polybutadiene by the manganese macrocycle is sequential, i.e., stepwise, processive or random processive. In the latter case the catalyst hops randomly from site to site during its action on the polymer chain eventually oxidizing all the alkene double bonds. If the threading speed of the macrocyclic catalyst on the polybutadiene chain is considered to be approximately 750 pm/s[6] and the speed of catalysis, as calculated from the catalyst turnover number, is ca. 1 pm/s,[5] the catalytic oxidation of polybutadiene by the manganese porphyrin macrocycle can be assumed to follow a random hopping mode, i.e., the random processive mechanism.[6]

In order to obtain a synthetic catalytic system that is capable of performing catalysis in a more sequential processive fashion, the translocation rate and the rate of the catalytic reaction need to be similar. This requires a system that displays either a slower translocation process or a faster catalytic reaction. Since the rate of catalysis is difficult to adjust, we chose for the first option and designed a porphyrin macrocycle that has a larger affinity for the polymer chain, which should lead to a slower translocation rate. We herein describe a new porphyrin cage compound **2** (Figure 1a), that has additional oxyethylene spacers in the glycoluril moiety, which results in a larger and more flexible cage structure compared to the previously reported porphyrin cage **1**. We present here the polymer threading studies on the flexible macrocycles $\mathbf{H_2}$ **2** and **Zn 2** and compare these with our previous findings on the porphyrin macrocycles $\mathbf{H_2}$ **1** and **Zn 1**. Threading studies on macrocycles **2** reveal a slower translocation process compared to macrocycles **1** as well as remarkable differences in polymer length dependency and energy profile of threading, which suggests that the manganese derivative of compound $\mathbf{H_2}$ **2** may be a promising candidate for achieving sequential processive catalysis.

Received: April 14, 2014

   dx.doi.org/10.1021/ja5032997 | J. Am. Chem. Soc. XXXX, XXX, XXX−XXX

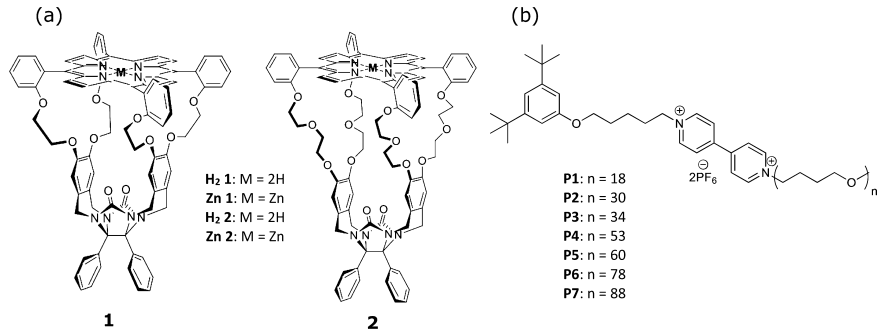

Figure 1. (a) Structures of porphyrin macrocycles. Left: rigid porphyrin **1** with four single oxyethylene spacers between the porphyrin and the glycoluril moiety. Right: porphyrin **2** with four bis(oxyethylene) spacers between the porphyrin and the glycoluril moiety. (b) Viologen-functionalized polytetrahydrofurans with different number of repeating units, which are used in the threading studies.

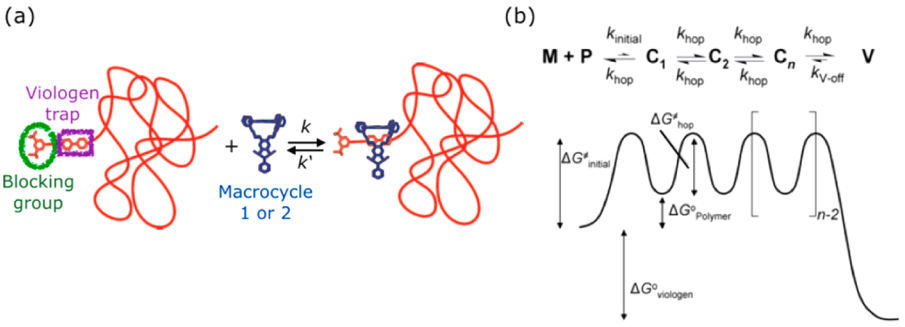

Figure 2. (a) Schematic representation of the (de)threading equilibrium; k describes the rate constant for threading, whereas k' is the rate constant for dethreading. (b) Energy diagram of the threading model with the rate constants (k) and energy levels of all the individual processes (M: macrocycle, P: polymer, V: viologen trap, C: local minimum).

RESULTS AND DISCUSSION

Previous Studies on Compound 1. In previous papers[6,7] we described a method for studying the threading of porphyrin cage compounds onto polymers of different length. To this end the polymers were blocked on one side with a di-*tert*-butylphenyl group and provided with a trap, i.e., a viologen molecule, which has a high affinity for the macrocyclic compound. The trap is located close to the blocking group and can only be reached by the porphyrin macrocycle if it first threads onto the open end of the polymer and then fully traverses the polymer chain (Figure 2a). Detailed analysis performed by NMR spectroscopy and MALDI-TOF mass spectrometry revealed the formation of only a 1:1 complex between porphyrin macrocycle and polymers under the conditions of the experiments.[6] The threading process can be followed by recording the fluorescence emission of the porphyrin, which is quenched when it reaches the viologen trap. This quenching only occurs when the viologen is bound inside the cavity. It was found that the threading process obeys second-order kinetics and the dethreading process follows first-order kinetics and that these processes are strongly dependent on the number of atoms of the thread, i.e., the length of the polymer chain. The threading kinetics were explained by using a consecutive-hopping mechanism (Figure 2b).[7,8]

In this model the threading is dependent on the initial binding event and the chance of arrival of the macrocycle at the viologen trap.[7] The overall threading rate constant k is described by $k = k_{initial}/(n + 1)$ and the overall dethreading rate constant k' by $k' = k_{v\text{-}off}/(n + 1)$. The rate constant for initial binding ($k_{initial}$) is independent of the length of the polymer chain, i.e., the number of atoms n, whereas the chance of arrival of the macrocycle to the viologen trap $(1/1 + n)$ is dependent on the polymer length. In the proposed consecutive-hopping mechanism the macrocycle finds the open end of the polymer and it "hops" from one local energy minimum to the other (Figure 2b).[7] Threading rates are usually high, and the association constant of the complexes between macrocycle **1** and the viologen traps of the polymers is $K_a = 10^7$ M^{-1}. The translocation speed of the macrocycle along the polymer chain is therefore not explicitly expressed in the consecutive-hopping model; however, it is statistically present in $n + 1$. Temperature-dependent measurements showed that the activation enthalpy of threading ($\Delta H^{\ddagger}$) is positive and remains constant, whereas the activation entropy ($\Delta S^{\ddagger}$) is negative and becomes more negative as the number of the atoms per chain increases. Thus, the energy barrier that has to be overcome for threading to occur is entropic in origin and depends on the length of the polymer chain.

Kinetics and Thermodynamics of Threading for Macrocycle 2. The target compounds $\mathbf{H_2}$ **2** and **Zn 2** were synthesized according to a published procedure.[9] The synthesis, characterization, and binding properties of these compounds will be described elsewhere.[9] Initial conformational analysis of macrocycle $\mathbf{H_2}$ **2** based on variable-temperature NMR, UV−vis spectroscopy, and computer modeling revealed that the flexible oxyethylene units are bent toward the inside of the cavity, which leads to a closed conformation at room temperature (Figure 3). At elevated temperatures, however, the oxyethylene units move away from the cavity leading to an open conformation, which will be discussed in the next sections.

Polymers **P1**−**P7** were synthesized as described previously.[7] The threading of $\mathbf{H_2}$ **2** onto polymers **P1**−**P7** was studied by fluorescence spectroscopy. Typically, to a known volume of $\mathbf{H_2}$ **2** ([$\mathbf{H_2}$ **2**](1 μM) in $CHCl_3/CH_3CN$, 1:1, v/v), 2.5 mol equiv

dx.doi.org/10.1021/ja5032997 | J. Am. Chem. Soc. XXXX, XXX, XXX−XXX

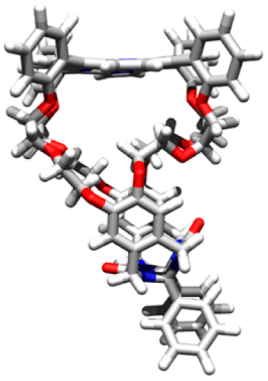

Figure 3. Computer-modeled structure of H_2 **2** in $CDCl_3$ at room temperature.[9]

of polymer solution was added at 296 K, and the fluorescence emission intensity of H_2 **2** was measured as a function of time. The fluorescence intensity decreased over time, indicating that the macrocycle finds the open end of the polymer and threads onto the polymer chain, eventually reaching the viologen trap, after which the fluorescence of the porphyrin is quenched (Figure 4a). A similar degree of fluorescence quenching was observed for each polymer at equilibrium, independent of the polymer length, which suggests that H_2 **2** binds to polymers **P1**−**P7** with similar association constants (*vide infra*, Table 1). While the trend in fluorescence quenching rate of H_2 **2** upon the addition of viologen-functionalized polymer is similar to that of H_2 **1** (i.e., the rate of quenching decreases as the polymer length increases), the degree of quenching is much lower in the case of H_2 **2**. The fraction of macrocycle−viologen complex in the mixture can be quantified by the decrease in fluorescence intensity. Addition of 2.5 equiv of polymer to H_2 **2** gives rise to only 25% decrease in fluorescence emission, while addition of 1 equiv of guest to H_2 **1** under identical conditions results in 75% fluorescence decrease (see the Supporting Information Figure S1 for **P2**). The association constants of the polymers and H_2 **2**, which were determined by applying second-order 1:1 kinetic binding isotherms (K_a = 10^5 M^{-1}, Table 1) (see the Supporting Information, part 3), revealed that H_2 **2** displays significantly lower affinities (K_a ~ 10^5 M^{-1}) for viologen derivatives **P1**−**P7** than H_2 **1** (K_a = 10^7 M^{-1}).[7] The threading experiments with H_2 **2** were further analyzed, and the rate constants of threading (k) and subsequently the free energy of activation for threading ($\Delta G^{\ddagger}$) were determined. The values of k and $\Delta G^{\ddagger}$ are depicted in Figure 4b,c as a function of number of atoms per polymer chain. The trend in the polymer length dependency of the k of H_2 **2** is different from that of the k of H_2 **1**, which in both cases shows a gradual shift from higher k to lower k (Figure 4b and Table 1). However, as the number of atoms in the polymer chain doubles (**P2**−**P5**) the rate of H_2 **2** decreases by a factor of 4, which is more than the expected factor of 2 predicted by the consecutive-hopping model for H_2 **1**. Presumably, the energy barrier associated with traversing the polymer chain upon increasing the polymer length increases more for H_2 **2** than it does for H_2 **1**. The initial threading event of H_2 **2** is apparently the rate-determining step for the short chain (**P1**-**P3**) threading process. However, when the chains are longer (**P4**-**P7**), the translocation step becomes the rate-determining step. We propose that the measured lower threading rates exhibited for the longer polymer chains are the result of a stronger affinity of the macrocycle for the polymer chain. Consequently, this leads to a slower translocation process, which becomes more pronounced for longer chains. Therefore, translocation becomes the rate-determining step in the overall threading process for longer chains, and this leads to deviations in the length dependency of threading of H_2 **2** as compared to H_2 **1**.

The experimental data depicted in Figure 4b,c could not be explained by using the conventional consecutive-hopping model. As mentioned above, the translocation process was not included in our previous model. In order to find out if the deviation is in fact the result of the translocation process and to fit the experimental data in Figure 4b,c better, we extended our model by adding a new parameter, $\Delta G^{\ddagger}_{translocation}$.

The free energy of activation of the threading ($\Delta G^{\ddagger}$), which is calculated from the measured rate constants, can be divided into three parts:

$$\Delta G^{\ddagger} = \Delta G^{\ddagger}_{initial} + \Delta G^{\ddagger}_{ca} + \Delta G^{\ddagger}_{translocation} \quad (1)$$

where $\Delta G^{\ddagger}_{initial}$ is the free energy of activation of initial binding, $\Delta G^{\ddagger}_{ca}$ is the additional free energy of activation corresponding to the length-dependent chance of arrival (ca) at the trap, and $\Delta G^{\ddagger}_{translocation}$ is the observed extra free energy of activation of the translocation process.

The individual free energy terms are given by eqs 2−4.

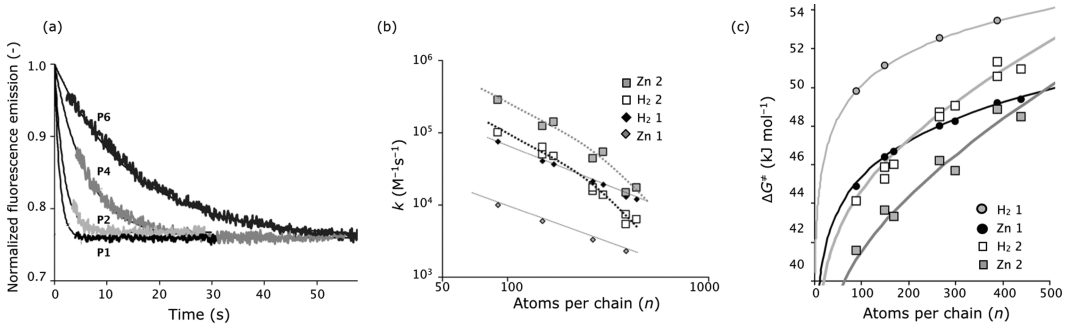

Figure 4. (a) Fluorescence emission intensity of H_2 **2** as a function of time upon addition of a polymer (2.5 equiv) (λ_{ex} = 426 nm, [H_2 **2**] = 1 μM in $CHCl_3/CH_3CN$, 1:1, v/v) at 296 K. For simplicity only experiments with **P1**, **P2**, **P4**, and **P6** are shown. The fits are obtained by 1:1 kinetic binding isotherms. (b) Rate constants for threading of macrocycles **Zn 2**, H_2 **2**, H_2 **1**, **Zn 1** as a function of the number of atoms per polymer chain. Fits are obtained by eq 1: $\Delta G^{\ddagger} = \Delta G^{\ddagger}_{initial} + \Delta G^{\ddagger}_{ca} + \Delta G^{\ddagger}_{translocation}$. (c) Free energy of activation of threading of macrocycles **Zn 2**, H_2 **2**, H_2 **1**, **Zn 1** as a function of atoms per polymer chain. The $\Delta G^{\ddagger}$ values are obtained from threading rate constants (k) using $\Delta G^{\ddagger} = -RT \ln(k h/k_B T)$ where R, k_B, and h, are the gas constant, Boltzmann constant, and Planck constant. (Estimated error = 5%.) Fits are obtained by eq 1.

dx.doi.org/10.1021/ja5032997 | J. Am. Chem. Soc. XXXX, XXX, XXX−XXX

Table 1. Thermodynamic and Kinetic Parameters for the Threading of H_2 2 onto P1−P7

polymer	no. of atoms	$k^{a,b}$ (M^{-1} s^{-1})	$\Delta G^{\ddagger}$ (kJ mol^{-1})	$\Delta H^{\ddagger c}$ (kJ mol^{-1})	$T\Delta S^{\ddagger c,e}$ (J mol^{-1} K^{-1})	$K_a^{a,b}$ (M^{-1})	ΔG° (kJ mol^{-1})	$\Delta H^{\circ d}$ (kJ mol^{-1})	$T\Delta S^{\circ d,e}$ (J mol^{-1} K^{-1})
P1	90	1.0×10^5	45	-19^e	-64^e	1.4×10^5	−29	−23	6
P2	150	5.6×10^4	46	-6^e	-52^e	1.2×10^5	−29	−23	6
P3	170	4.7×10^4	47	-27^f	-74^f	1.3×10^5	−29	−30	0
P4	266	1.6×10^4	49	-3^e	-52^e	1.4×10^5	−29	−23	7
P5	300	1.4×10^4	49	-17^f	-67^f	1.4×10^5	−29	−28	1
P6	390	6.4×10^3	51	8^e	-43^e	1.4×10^5	−29	−26	3
P7	440	6.3×10^3	51	-14^f	-65^f	1.5×10^5	−29	−31	−1

[a] T = 296 K. [b] Estimated error = 30%. [c] Estimated error = ±15 kJ mol^{-1}. [d] T = 298 K, estimated error = ±3 kJ mol^{-1}. [e] [H_2 2] = 1.5 μM. [f] [H_2 2] = 0.6 μM.

$$\Delta G^{\ddagger}_{\text{initial}} = -RT\ln(k_{\text{initial}} \times h/k_B T) \quad (2)$$

$$\Delta G^{\ddagger}_{\text{ca}} = RT\ln(n+1) \quad (3)$$

$$\Delta G^{\ddagger}_{\text{translocation}} = n \times \Delta G^{\ddagger}_{\text{atom}} \quad (4)$$

Equations 2 and 3 follow directly from the conventional consecutive-hopping model,[7] and eq 4 provides the free energy of activation of traversing a single atom $\Delta G^{\ddagger}_{\text{atom}}$ on the polymer chain by the porphyrin macrocycle, where n is the number of atoms in the polymer chain. $\Delta G^{\ddagger}_{\text{atom}}$ is an additional parameter to describe the deviations of the threading of **H_2 2** from the conventional consecutive-hopping model, which holds for **H_2 1**. Fits obtained by eq 1 are in good agreement with the experimental data (see Figure 4b,c). From the measured values of $\Delta G^{\ddagger}$ (Table 1) the values for k_{initial} and $\Delta G^{\ddagger}_{\text{atom}}$ were calculated using eqs 1−4. The results are presented in Table 2.

Table 2. Rate Constants for Initial Binding and the Apparent Extra Free Energy of Activation $\Delta G^{\ddagger}_{\text{atom}}$ Resulting from the Translocation Process (T = 296 K)

macrocycle	k_{initial} (M^{-1} s^{-1})[a]	$\Delta G^{\ddagger}_{\text{atom}}$ (J mol^{-1})[b]
H_2 1	6.5×10^6	1.5
Zn 1	9.0×10^5	0
H_2 2	1.2×10^7	9.5
Zn 2	4.7×10^7	12.5

[a] Estimated error = 50%. [b] Estimated error = 30% (average of fitting using all polymers).

H_2 2 and **Zn 2** display additional $\Delta G^{\ddagger}_{\text{atom}}$ values of 9.5 and 12.5 J mol^{-1}, respectively, as a result of their slow translocation speed (i.e., additional binding−releasing events through the polymer chain). For **H_2 1** and **Zn 1**, in which slow translocation is not observed, these numbers are 1.5 and 0 J mol^{-1}, respectively.

In separate experiments we investigated the effect of temperature on the threading rate by monitoring the fluorescence quenching at different temperatures and determined the rate constant k for threading of **H_2 2**. Our findings showed that the threading rate decreases upon increasing temperature (see the Supporting Information, Figure S2). The rate of chemical reactions usually increases with increasing temperature;[10] however the different behavior observed here is the result of the conformational changes exhibited by **H_2 2**, which will be discussed below. From the temperature-dependent threading experiments also the enthalpic ($\Delta H^{\ddagger}$) and entropic ($\Delta S^{\ddagger}$) contributions to the free energy of activation of threading ($\Delta G^{\ddagger}$) for **H_2 2** for each polymer were obtained by constructing Eyring plots (see the Supporting Information, Figure S2). Although slight changes in concentrations of the samples resulted in significant deviations, some clear trends could be observed (Table 1 and Figure 5a). The activation enthalpy ($\Delta H^{\ddagger}$) is negative for each sample (except for **P6**)[11] and becomes more positive as the number of atoms per polymer chain increases. On the other hand, the $T\Delta S^{\ddagger}$ values are negative and reveal a slight trend to become less negative upon increasing the number of atoms per polymer chain. Figure 5a shows the activation parameters as a function of the number of atoms in the polymer chains and the corresponding fits obtained by eq 1. The experimental and theoretical data are in good agreement for $\Delta G^{\ddagger}$ (black line) but scatter quite a bit for the individual activation parameters $\Delta H^{\ddagger}$

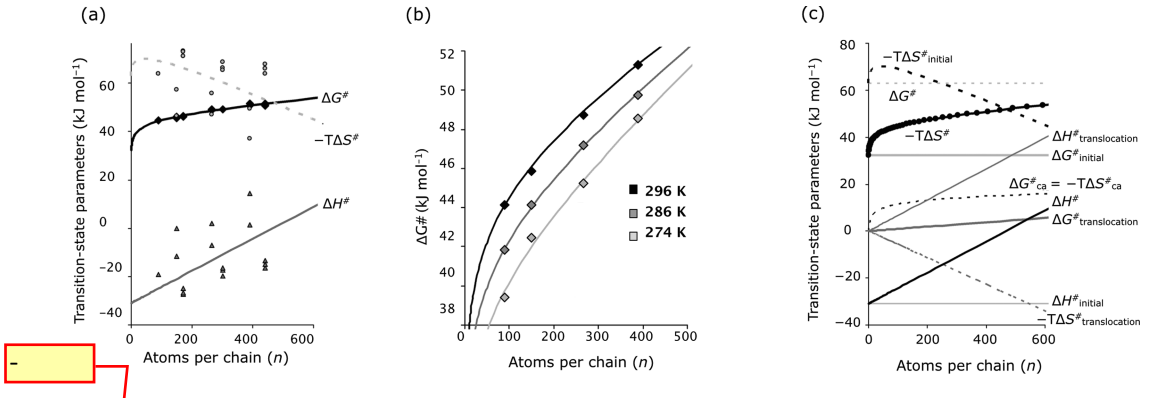

Figure 5. Transition state parameters for threading of **P1−P7** through **H_2 2** as a function of number of atoms per polymer chain with corresponding fits by using eq 1 ([**H_2 2**] = 1 μM in $CHCl_3$:CH_3CN, 1:1 v/v). (a) Experimentally obtained values, T = 296 K. (b) $\Delta G^{\ddagger}$ as a function of number of atoms per polymer chain at different temperatures. (c) Theoretically obtained thermodynamic parameters according to eq 1, T = 296 K.

dx.doi.org/10.1021/ja5032997 | J. Am. Chem. Soc. XXXX, XXX, XXX−XXX

Table 3. Thermodynamic and Kinetic Parameters for the Threading of Zn 2 onto P1−P7

polymer	no. of atoms	k_{on} [a,b] ($M^{-1}s^{-1}$)	$\Delta G^{\ddagger}_{on}$	$\Delta H^{\ddagger}_{on}$ [c]	$T\Delta S^{\ddagger}_{on}$ [c]	K_a [b] (M^{-1})	$\Delta G^{\circ}_{overall}$ [d]
P1	90	2.9×10^5	42	−8	−50	3.0×10^5	−31
P2	150	1.2×10^5	44	−3	−47	3.1×10^5	−31
P3	170	1.4×10^5	43	n.d.	n.d.	3.2×10^5	−31
P4	266	4.3×10^4	46	2	−44	3.5×10^5	−31
P5	300	5.4×10^4	46	n.d	n.d.	3.6×10^5	−31
P6	390	1.5×10^4	49	3	−46	3.6×10^5	−31
P7	440	1.7×10^4	49	n.d.	n.d.	3.3×10^5	−31

[a] T = 296 K. [b] Estimated error = 20%. [c] Estimated error = ±15 kJ mol^{-1}. [d] T = 298 K, estimated error = ±3 kJ mol^{-1}.

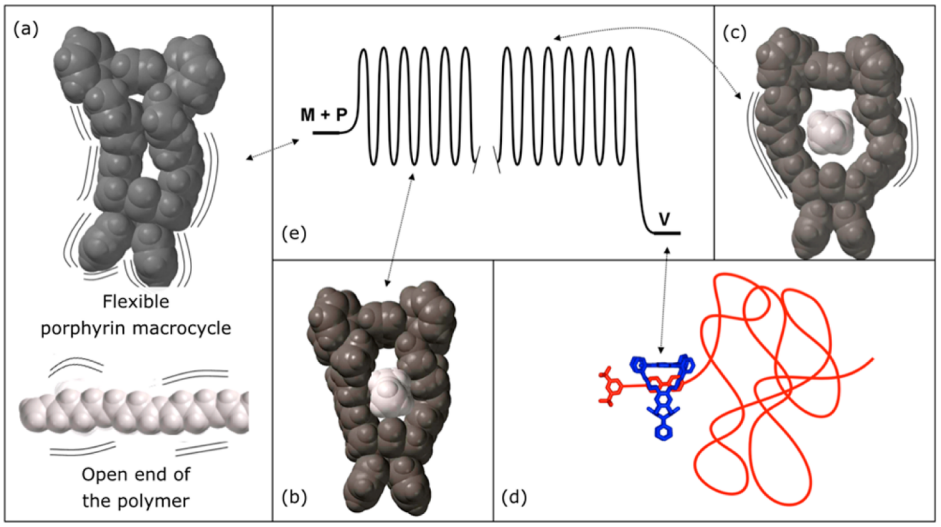

Figure 6. General threading mechanism of polymers through flexible porphyrin macrocycles. Energy minimalized structures of (a) macrocycle H_2 **2** (top) and the open end of a viologen-functionalized polymer (bottom) when they are free in solution. (b) Initial binding of the open end of the polymer chain to H_2 **2** via an induced-fit mechanism. (c) Translocation of H_2 **2** along the polymer chain. (d) Schematic representation of macrocycle H_2 **2** reaching the viologen trap. The process eventually reaches a thermodynamic sink. (e) Energy landscape describing the threading process of polymers through H_2 **2** according to the consecutive-hopping model.

(gray line) and $T\Delta S^{\ddagger}$ (dashed line) because of the large errors involved. The fits show the trend in the energy profiles, i.e., an decrease in the $-\Delta S^{\ddagger}$ and an increase in $\Delta H^{\ddagger}$ as a function of the number of atoms in a polymer chain, as derived from Table 1. The results suggest that the threading of H_2 **2** becomes entropically favorable and enthalpically unfavorable as the length of the polymer chain increases. The data obtained for macrocycle H_2 **2** and polymers **P1**−**P7** are remarkably different from those observed for the threading of H_2 **1** onto **P1**−**P7** under identical conditions. The activation enthalpy of threading for H_2 **1** is positive, $\Delta H^{\ddagger}$ = +20 kJ mol^{-1}, and remains constant as the number of atoms per polymer chain increases. Furthermore, the value of $T\Delta S^{\ddagger}$ becomes more negative (from −15 to −29 kJ mol^{-1}) as the chain length increases (i.e., threading becomes more entropically unfavorable as the chain length increases), which is in agreement with the consecutive-hopping model.[7]

In order to better comprehend the transition-state parameters displayed in Figure 5a, the energy of activation for threading, $\Delta G^{\ddagger}$, was analyzed as a function of number of atoms per polymer chain at three different temperatures (Figure 5b). By using the fits obtained in Figure 5b the values for $k_{initial}$, $\Delta G^{\ddagger}_{atom}$, and subsequently the activation parameters, $\Delta H^{\ddagger}_{initial}$, $\Delta S^{\ddagger}_{initial}$, $\Delta H^{\ddagger}_{atom}$, and $\Delta S^{\ddagger}_{atom}$ were derived (Figure 5c). For macrocycle H_2 **2** and polymer **P1** the value of $k_{initial}$ increases upon lowering the temperature ($k_{initial}$ = 1.4×10^7 M^{-1} s^{-1} at 296 K, $k_{initial}$ = 3.5×10^7 M^{-1} s^{-1} at 274 K), indicating that the initial binding of H_2 **2** to the open end of **P1** is faster at lower temperatures. This consequently results in a negative activation enthalpy ($\Delta H^{\ddagger}_{initial}$ = −31 ± 10 kJ mol^{-1}) and a negative activation entropy ($T\Delta S^{\ddagger}_{initial}$ = −63 ± 10 kJ mol^{-1}), suggesting that the initial binding is enthalpically favorable and entropically highly unfavorable. Furthermore, the values derived for $\Delta G^{\ddagger}_{atom}$ at different temperatures revealed that $\Delta G^{\ddagger}_{atom}$ increases upon decreasing temperature. ($\Delta G^{\ddagger}_{atom}$ = 9.4 J mol^{-1} at 296 K, $\Delta G^{\ddagger}_{atom}$ = 13.6 kJ mol^{-1} at 276 K). Apparently, the energy barrier for translocation is higher at lower temperatures, leading to a slower translocation process at lower temperatures. From the values of $\Delta G^{\ddagger}_{atom}$ at different temperatures the values for $\Delta H^{\ddagger}_{atom}$ (66 ± 20 J mol^{-1}) and $T\Delta S^{\ddagger}_{atom}$ (57 ± 20 J mol^{-1}) were calculated. The obtained values indicate that for H_2 **2** the translocation process is entropically driven and enthalpically unfavorable.

In a separate set of experiments we performed temperature-dependent threading measurements in order to determine the enthalpic (ΔH°) and entropic (ΔS°) contributions to the free energy of binding (ΔG°). Association constants for complexes between H_2 **2** and **P1**−**P7** at equilibrium were determined at different temperatures and thermodynamic parameters were obtained by using Van't Hoff plots (see Supporting Information Figure S3). As depicted in Table 1, the enthalpy of binding for complex formation between H_2 **2** and **P1**−**P7** has a value ranging from ΔH° = −23 to −31 kJ mol^{-1} while the entropic contribution ranges from $T\Delta S^{\circ}$ = 7 to −1 kJ mol^{-1}. This

dx.doi.org/10.1021/ja5032997 | J. Am. Chem. Soc. XXXX, XXX, XXX−XXX

indicates that the free energy of binding ΔG° (= −30 kJ mol^{-1} for **P4**) is mainly the result of a favorable binding enthalpy. Thermodynamic parameters observed for complexes of $\mathbf{H_2}$ **2** with **P1**−**P7** complexes deviate significantly from the ones obtained for complexes of $\mathbf{H_2}$ **1** with **P1**−**P7**. Typical thermodynamic parameters for complexes with $\mathbf{H_2}$ **1** amounted to ΔH° = −19 kJ mol^{-1} and $T\Delta S^\circ$ = 21 kJ mol^{-1}, which yields a free energy of binding ΔG° = −40 kJ mol^{-1}.[7] In this case, enthalpic and entropic parameters contribute almost equally to ΔG°.

Threading of Zn 2. The threading of **Zn 2** over polymers **P1**−**P7** was studied in a similar way as for $\mathbf{H_2}$ **2**. Analysis of the data revealed that the k values for threading of **Zn 2** are on average 2.9 times higher than those of $\mathbf{H_2}$ **2** (compare Table 1 with Table 3). This observed threading behavior is in contrast to the behavior observed for $\mathbf{H_2}$ **1** and **Zn 1** in which threading of $\mathbf{H_2}$ **1** is faster than that of **Zn 1**. This difference could be the result of the coordination of the zinc center of **Zn 2** to the oxygen atoms in the oxyethylene moieties of the host (see the Supporting Information, Figure S6). The polymer length-dependency of the threading process of **Zn 2**, however, is similar to that observed for $\mathbf{H_2}$ **2** and also the calculated activation parameters revealed similar values and length dependencies. **Zn 2** showed a higher threading rate with decreasing temperature similar to $\mathbf{H_2}$ **2**. Furthermore, a negative and increasing (more positive) value for $\Delta H^\ddagger$ and a negative and increasing (less negative) value of $T\Delta S^\ddagger$ as a function of the number of atoms in the polymer chain were observed (Table 3).

Mechanism of Threading. The mechanism proposed for the threading process of $\mathbf{H_2}$ **2** is presented in Figure 6. The initial binding of the macrocycle to the open end of the polymer chain is entropically highly unfavorable ($T\Delta S^\ddagger_{\text{initial}}$ = −63 ± 10 kJ mol^{-1}), which can be attributed to the loss of conformational freedom of both the flexible cavity and the open end of the polymer chain upon binding (Figure 6a). Once threaded, $\mathbf{H_2}$ **2** moves along the polymer chain randomly, "hopping" from one local energy minimum to the other (Figure 6b,e). The derived values for $\Delta H^\ddagger_{\text{atom}}$ (66 ± 20 J mol^{-1}) and $\Delta S^\ddagger_{\text{atom}}$ ($T\Delta S^\ddagger_{\text{atom}}$ = 57 ± 20 J mol^{-1}) indicate that the translocation process is entropically favorable and enthalpically unfavorable. This is unprecedented because one would expect that the movement along the polymer requires the stretching and ordering of the polymer chain, which is entropically unfavorable. The experimental observations, on the other hand, suggest that $\mathbf{H_2}$ **2** has a relatively strong affinity for the chain, which leads to the conclusion that the translocation process becomes a more rate-determining factor than the rearrangement of the polymer chain. In order to translocate along the chain, $\mathbf{H_2}$ **2** first has to adopt a more relaxed conformation in which it releases the tight binding geometry with the chain (Figure 6c,e), which is an enthalpically unfavorable but entropically favorable process. This results in a more positive $\Delta H^\ddagger$ and a less negative $\Delta S^\ddagger$ upon increasing polymer lengths, and because of this the translocation process becomes significantly more apparent in the threading process upon increasing chain length (as observed in the rate of quenching in fluorescence emission). Finally, the macrocycle $\mathbf{H_2}$ **2** reaches the viologen trap and the system relaxes to find its energy minimum (Figure 6d,e). The chance of reaching the viologen is proportional to the polymer chain length. For $\mathbf{H_2}$ **1** and **Zn 1**, where the translocation process is not expressed in the threading curves (as observed in the rate of quenching of the fluorescence emission) only the chance of arrival determines the observed length dependency, and this is expressed in extra activation entropy upon increasing chain lengths. This entropic effect is not observed for threading of polymers through $\mathbf{H_2}$ **2** because it is compensated for by the entropically favorable translocation process.

The measured negative enthalpy of activation for the threading (e.g., $\Delta H^\ddagger$ = −19 kJ mol^{-1} for the combination $\mathbf{H_2}$ **2** and **P1**, Table 1) and for the initial binding event (for $\mathbf{H_2}$ **2** $\Delta H^\ddagger_{\text{initial}}$ = −31 ± 10 kJ mol^{-1}, see above) is highly uncommon in supramolecular systems.[12,13] The rate of complexation reported for various comparable synthetic supramolecular systems decreases upon lowering the temperature, and these processes all have positive activation enthalpies.[14−17] In some protein systems, however, negative activation enthalpies for binding processes have been reported,[18−20] and these are mostly associated with protein folding. Furthermore, a number of reactions including Diels−Alder reactions,[21] radical reactions,[22] and proton-[23] and electron-transfer reactions[24] display negative activation enthalpies.[25]

For $\mathbf{H_2}$ **2**, the observed negative $\Delta H^\ddagger$ can be explained by its specific conformational behavior. $\mathbf{H_2}$ **2** adopts a geometry in which the oxyethylene spacers fill the space in between the glycoluril moiety and the porphyrin. Variable-temperature ^{1}H NMR experiments showed a strong downfield shift of the oxyethylene spacer protons, suggesting that these protons move away from the proximity of the porphyrin ring upon lowering the temperature, which leads to a wider cavity (see the Supporting Information, Figure S5). Therefore, the binding of the open end of the polymer chain to the cavity becomes easier at lower temperatures. The observed increase in initial threading rate at lower temperatures and the negative $\Delta H^\ddagger$ may be a result of the conformational change in the molecule. The initial binding therefore has an entropic penalty; however, it is enthalpically driven.

Theoretical Evaluation. As mentioned above we used the consecutive-hopping model to explain the mechanism of threading for regular porphyrins[7] and we extended this model in order to describe the threading mechanism of macrocycles $\mathbf{H_2}$ **2** and **Zn 2**. This model also allows us to simulate threading curves for polymers with different chain-lengths and macrocycles with a larger affinity for the polymer chain. By using these simulations, we may describe the deviations in the threading kinetics of compounds **2** compared to compounds **1** and verify the presence of a slow translocation process in the threading of the first mentioned compounds.

We previously proposed that the observed chain-length dependency of the threading process originates from the rate of initial binding of the first few atoms of the polymer chain into the cavity of the macrocycle (called entron) and the chance of arrival of the macrocycle at the viologen trap.[7] The relative rates of initial binding and the movement along the chain can be calculated, but the absolute magnitudes of k_{hop} (the rate constant of "hopping" of the macrocycle from one energy minimum to another) and $k_{\text{entron-off}}$ (the rate constant of the macrocycle leaving the chain) are unknown, and it is therefore not possible to derive the value of the movement rate along the chain. In order to estimate the relative magnitudes of k_{hop} and the number of steady-state intermediates n (local energy minima), we extended our model. The two events in the threading process, i.e., the initial binding to the open end of the chain and the movement along the chain, will be treated separately, and expressed in terms of half-life times ($t_{1/2}$).

dx.doi.org/10.1021/ja5032997 | J. Am. Chem. Soc. XXXX, XXX, XXX−XXX

Table 4. Half-life Times for the Initial Binding Event ($t_{1/2\text{-entron}}$) and the Translocation Process ($t_{1/2\text{-translocation}}$) As a Function of the Number of Local Energy Minima (n) and the Rate Constant of the Hopping Steps (k_{hop})

	k_{entron} (M^{-1} s^{-1})	k_{hop} (s^{-1})					
	5×10^6	1×10^7	1×10^6	1×10^5	1×10^4	1×10^3	1×10^2
n	$t_{1/2\text{-entron}}$ (s)	$t_{1/2\text{-translocation}}$ (s)					
67	0.2	9×10^{-5}	9×10^{-4}	9×10^{-3}	9×10^{-2}	**0.9**	**8.5**
125	0.2	2×10^{-4}	2×10^{-3}	2×10^{-2}	**0.2**	**2.5**	**25**
250	0.2	8×10^{-4}	8×10^{-3}	8×10^{-2}	**0.8**	**8.1**	**8.1**
500	0.2	3×10^{-3}	3×10^{-2}	**0.3**	**2.7**	**27**	**267**
1000	0.2	9×10^{-3}	8×10^{-2}	**0.9**	**8.8**	**88**	**884**

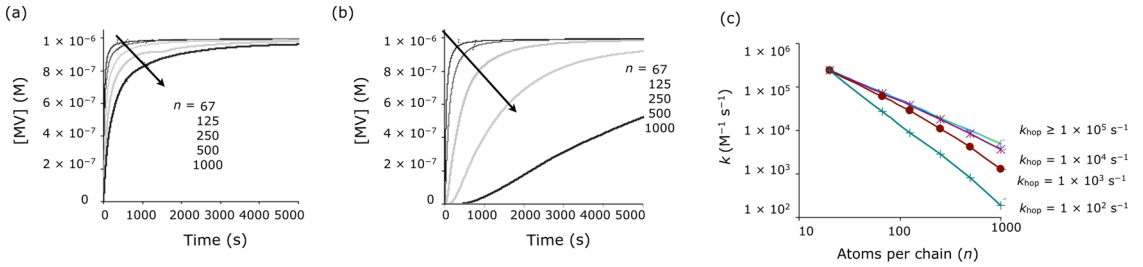

Figure 7. Simulated threading curves. Concentration of macrocycle−viologen complex (MV) as a function of time for different values of n (local energy minima). The arrows show increasing n. (a) Macrocycle has little affinity for the polymer chain ($k_{entron} = 5 \times 10^6$ M^{-1} s^{-1}, $k_{hop} = 1 \times 10^7$ s^{-1}). (b) Macrocycle has strong affinity for the chain ($k_{entron} = 5 \times 10^6$ M^{-1} s^{-1}, $k_{hop} = 1 \times 10^2$ s^{-1}). (c) Threading rate constant as a function of polymer chain length (n) for different values of k_{hop}. As the affinity for the chain increases (i.e., k_{hop} decreases) the observed length dependency deviates from the length dependency according to equation $k = k_{initial}/n + 1$ (curve for $k_{hop} \geq 1 \times 10^5$).

The initial binding of the macrocycle to the open end of the chain is a second-order process. Furthermore, the threading rates depend on the macrocycle and polymer concentration ($[P_o]$). The time for binding half of the concentration of macrocycle to the open end of the polymer chain ($t_{1/2\text{-entron}}$) is given by eq 5.

$$t_{1/2\text{-entron}} = 1/(k_{entron}[P]_o) \quad (5)$$

First, we calculated $t_{1/2\text{-translocation}}$, which is the time for the arrival of half of the macrocycles at the viologen trap with different values of n and k_{hop}. Then we compared these values with $t_{1/2\text{-entron}}$, which can be calculated from the values of k_{entron} and $[P_o]$ by using eqs 1 and 2 ($k_{entron} = k_{initial}$, *vide supra*) and eq 5. When $k_{entron} < k_{hop}$, the macrocycle has an interaction with the polymer chain that can be expressed by $K_{Polymer} = k_{hop}/k_{entron}$, which is higher than 1 M^{-1}, and the interaction with the polymer chain is therefore weak. Table 4 shows that when $K_{Polymer} = k_{hop}/k_{entron} > 1$ M^{-1}, $t_{1/2\text{-entron}}$ for values of n up to 1000 is significantly larger than $t_{1/2\text{-translocation}}$. The translocation is therefore significantly faster than the initial binding event. As a result, the overall threading curves depend only on the initial binding rate and the chance of arrival (ca). On the other hand, when $K_{Polymer} = k_{hop}/k_{entron} < 1$, $t_{1/2\text{-translocation}}$ becomes of the same order of magnitude as, or even higher than $t_{1/2\text{-entron}}$, depending on the values of k_{hop} and n. In that case the translocation process plays a significant role in the observed overall threading curves. A number of simulations for threading of a macrocycle with weaker or stronger affinities for the polymer chain are depicted in Figure 7a,b, respectively.

The simulations show that when the affinity for the polymer chain increases (lower k_{hop}), the curves deviate upon increasing n (Figure 7b). The translocation thus becomes apparent in the overall threading curves, which is expressed in slower evolution of the complex formation, but also in the appearance of sigmoid curve shapes. As depicted in Table 4 the deviations become apparent when $t_{1/2\text{-translocation}}$ equals $t_{1/2\text{-entron}}$ and become larger when $t_{1/2\text{-translocation}} > t_{1/2\text{-entron}}$. As soon as the threading curves become sigmoidal, showing an initial delay before fluorescence quenching is observed, the overall threading curves can no longer be fitted to 1:1 binding kinetics, and the threading-on process is no longer purely second-order. Given that the initial delay lies within the initial part of the curves, which is in most cases during the experimental mixing time of the components, these deviations from perfect 1:1 binding kinetics might experimentally not be directly apparent.

Threading rate constants were also calculated at different polymer concentrations. At increasing polymer concentrations, $t_{1/2\text{-entron}}$ decreases, whereas $t_{1/2\text{-translocation}}$ remains constant because the latter is an overall first-order process and therefore concentration independent. As a result, the deviation from the 1:1 binding kinetics is expressed to a larger extent at higher polymer concentration. An increasing affinity of the macrocycle for the polymer chain also starts to influence the observed association equilibrium constant for the viologen moiety. In that case the binding to the chain competes with the binding to the viologen, and it can therefore be expected that increasing chain lengths would result in less binding to the viologen (hence less fluorescence quenching and lower apparent association equilibrium constants). This may also result in the formation of polyrotaxane species in which several macrocycles are threaded onto a single chain,[26−30] which would dramatically complicate the consecutive hopping model. A general equation for the observed length dependency of the threading process is therefore as given in eq 6, where f is an additional factor larger than 1 that depends on n and the affinity of the macrocycle for the polymer.

$$k = k_{initial}/(n + 1)f \quad (6)$$

According to this equation the threading rate is halved as the polymer chain length increases 2-fold. When the macrocycle

dx.doi.org/10.1021/ja5032997 | J. Am. Chem. Soc. XXXX, XXX, XXX−XXX

has a larger affinity for the polymer chain the rate decrease is even larger upon doubling the polymer chain length (Figure 7c).

CONCLUSIONS

From the results presented above we may conclude that the length dependency and the energy profiles of the process of threading polymers through macrocycles **2** are remarkably different from those of the smaller and more rigid macrocycles **1**. Macrocycle **2** has a stronger affinity for the polymer chain, most likely as a result of induced-fit binding effects, leading to a slower translocation process, which is expressed in the overall threading rate curves. Interestingly, the initial binding of $\mathbf{H_2}$ **2** to the polymer chain has a favorable negative enthalpy of activation which is probably related to the opening of the cavity at lower temperatures. The translocation process along the chain, on the other hand, is enthalpically unfavorable, which can be ascribed to the release of the tight binding to the chain upon translocation, and entropically favorable. The threading of zinc derivative **Zn 2** is faster than that of $\mathbf{H_2}$ **2**, which is in contrast to our previous studies with **Zn 1**, for which the kinetics of threading was shown to be slower compared to its free base derivative $\mathbf{H_2}$ **1**. The reason for this remains unanswered; however, our findings suggest that the initial threading process may have a different mechanism, and the rate of initial complex formation between the polymer chain and the flexible cavity is probably determined by very subtle differences in the properties of the host cavity, for instance the internal binding and release of the spacer oxygen atoms, which may be different for **Zn 2** when compared to $\mathbf{H_2}$ **2**.

One of the objectives of this study was to design a catalytic host system that would move more slowly along a polymer chain than the previously reported systems. This would lead to a better match between movement and coupled catalysis, e.g., movement and epoxidation of a polybutadiene chain. The outcome of the present study shows that this can be achieved by a simple elongation of the spacer groups between the diphenylglycoluril host and the porphyrin catalyst. This means the catalytic host wraps itself around the polymer chain, thereby slowing down its movement. We are planning catalytic studies to see whether the present modification of the catalytic host indeed results in a stepwise processive catalysis process. These studies will be published in due course.

ASSOCIATED CONTENT

Supporting Information

General experimental protocols, additional fluorescence measurements for threading of $\mathbf{H_2}$ **1** and $\mathbf{H_2}$ **2**, conformational analysis of macrocycle $\mathbf{H_2}$ **2** by NMR and UV−vis spectroscopy, 1:1 kinetic binding model and simulations. This material is available free of charge via the Internet at http://pubs.acs.org.

AUTHOR INFORMATION

Corresponding Authors

a.rowan@science.ru.nl

r.nolte@science.ru.nl

Notes

The authors declare no competing financial interest.

ACKNOWLEDGMENTS

This research was supported by the European Research Council in the form of an ERC Advanced grant to R.J.M.N. (ALPROS-290886) and an ERC Starting grant to J.A.A.W.E (NANOCAT-259064). Further financial support was obtained from the Council for the Chemical Sciences of The Netherlands Organization for Scientific Research (CW-NWO) (Vidi grant for J.A.A.W.E and Vici grant for A.E.R) and from the Ministry of Education, Culture and Science (Gravity program 024.001.035).

REFERENCES

(1) Wickner, W.; Schekman, R. *Science* **2005**, *310*, 1452.
(2) Wente, S. R. *Science* **2000**, *288*, 1374.
(3) Breyer, W. A.; Matthew, B. M. *Protein Sci.* **2001**, *10*, 1699.
(4) Kool, E. T.; Morales, J. C.; Guckian, K. M. *Angew. Chem., Int. Ed.* **2000**, *39*, 990.
(5) Thordarson, P.; Bijsterveld, E. J. A.; Rowan, A. E.; Nolte, R. J. M. *Nature* **2003**, *424*, 915.
(6) Coumans, R. G. E.; Elemans, J. A. A. W.; Nolte, R. J. M.; Rowan, A. E. *Proc. Natl. Acad. Sci. U.S.A.* **2006**, *103*, 19647.
(7) Deutman, A. B. C.; Monnereau, C.; Elemans, J. A. A. W.; Ercolani, G.; Nolte, R. J. M.; Rowan, A. E. *Science* **2008**, *322*, 1668.
(8) Herrmann, W.; Keller, B.; Wenz, G. *Macromolecules* **1997**, *30*, 4966.
(9) Deutman, A. B. C.; Smits, J. M. M.; de Gelder, R.; Elemans, J. A. A. W.; Nolte, R. J. M.; Rowan, A. E. *Chem. Eur. J.*, in press.
(10) Connors, K. A. *Chemical Kinetics: The Study of Reaction Rates in Solution*; VCH: New York, 1990.
(11) Slight changes in concentrations of the samples resulted in some deviations from the trend.
(12) Fang, L.; Basu, S.; Sue, C.- H.; Fahrenbach, A. C.; Stoddart, J. F. *J. Am. Chem. Soc.* **2011**, *133*, 396.
(13) Xu, Y.; Xu, W. L.; Smith, M. D.; Shimizu, L. S. *RSC Adv.* **2014**, *4*, 1675.
(14) Affeld, A.; Hubner, G. M.; Seel, C.; Schalley, C. A. *Eur. J. Org. Chem.* **2001**, 2877.
(15) Linnartz, P.; Bitter, S.; Schalley, C. A. *Eur. J. Org. Chem.* **2003**, 4819.
(16) Assava, M.; Ashton, P. R.; Ballardini, R.; Balzani, V.; Belohradsky, M.; Gandolfi, M. T.; Kocian, O.; Prodi, L.; Raymo, F. M.; Stoddart, J. F.; Venturi, M. *J. Am. Chem. Soc.* **1997**, *119*, 302.
(17) Raymo, F. M.; Stoddart, J. F. *Pure Appl. Chem.* **1997**, *69*, 1987.
(18) Oliveberg, M.; Tan, Y.-J.; Fersht, A. R. *Proc. Natl. Acad. Sci. U.S.A.* **1995**, *92*, 8926.
(19) Schneider, W. *Proc. Natl. Acad. Sci. U.S.A.* **1979**, *76*, 2283.
(20) Meliga, S. C.; Farrugia, W.; Ramsland, P. A.; Falconer, R. J. *J. Phys. Chem. B* **2013**, *117*, 490.
(21) Kiselev, V. D.; Miller, J. G. *J. Am. Chem. Soc.* **1975**, *97*, 4036.
(22) Wang, J.; Doubleday, C., Jr.; Turro, N. J. *J. Am. Chem. Soc.* **1989**, *111*, 3962.
(23) Reitstoen, B.; Parker, V. D. *J. Am. Chem. Soc.* **1990**, *112*, 4968.
(24) Kapinus, E. I.; Rau, H. *J. Phys. Chem. A* **1998**, *102*, 5569.
(25) Frank, R.; Greiner, G.; Rau, H. *Phys. Chem. Chem. Phys.* **1999**, *1*, 3481.
(26) Zhang, W.; Dichtel, W. R.; Stieg, A. Z.; Benitez, D.; Gimzewski, J. K.; Heath, J. R.; Stoddart, J. F. *Proc. Natl. Acad. Sci. U.S.A.* **2008**, *105*, 6514.
(27) Wu, J.; Leung, K. C.-F.; Stoddart, J. F. *Proc. Natl. Acad. Sci. U.S.A.* **2007**, *104*, 17266.
(28) Osaki, M.; Takashima, Y.; Yamaguchi, H.; Harada, A. *J. Am. Chem. Soc.* **2007**, *129*, 14452.
(29) Wenz, G.; Han, B. H.; Müller, A. *Chem. Rev.* **2006**, *106*, 782.
(30) Daniell, H. W.; Klotz, E. J. F.; Odell, B.; Claridge, T. D. W.; Anderson, H. L. *Angew. Chem., Int. Ed.* **2007**, *46*, 6845.